"CORT-EX:" A Program for Quantitative Analysis of Brain SPECT Data

Guy Lamoureux, Renee M. Dupont, William L. Ashburn, and Samuel E. Halpern

Département de Médecine Nucléaire et Radiobiologie, Université de Sherbrooke, Sherbrooke, P. Québec, Canada; Department of Psychiatry, Veterans Administration Medical Center and University of California, San Diego, California; Department of Nuclear Medicine, Veterans Administration Medical Center, San Diego, California; and Division of Nuclear Medicine, University of California, San Diego, California

A program was developed to extract from brain SPECT data global as well as regional concentrations of a radiopharmaceutical while allowing for improved subjective evaluation of its distribution. This program was used to process the data obtained from 17 normal subjects, 20 min, 2 hr, and 4 hr after the injection of iodine-labeled iodoamphetamines. The mean absolute cortical uptake at these three time periods was 0.921 (±0.185), 0.803 (±0.107), and 0.748 (±0.103) in arbitrary units (±s.d.), respectively. The regional distribution of the tracer became more uniform with time due to an uneven washout rate. The cerebellum was noted to have a very high variability in its uptake and a high washout rate, making it unsuitable as an internal standard for relative quantification. Finally, a repeat study was performed on 10 subjects. No significant difference could be demonstrated in the mean uptake of the group at 2 and 4 hr, however the difference observed in the 20 min uptake values was significant at the p = 0.05 level.

J Nucl Med 1990; 31:1862–1871

With the approval by the FDA of some new brain imaging agents (*1–2*), and many more in development (*3–5*), brain imaging appears to be on the verge of making a comeback in nuclear medicine. Among these agents, those directed toward the determination of brain blood flow are probably the best known. Iodine-123-iodoamphetamine ([^{123}I]IMP), a "blood-flow" agent, has been studied by several investigators and was found to be of possible value in stroke (*6–8*), epilepsy (*9–10*), and dementia (*11–12*), to name a few. However, its clinical effectiveness seems to be heavily dependant on the availability of single-photon emission computed tomography (SPECT) due to its unique ability (versus planar imaging) to provide contrast between the structures of the brain located at various depths. This communication describes a new technique for the analysis of brain SPECT data that can be used to generate quantitative uptake maps of the brain. This program can facilitate the interpretation of the data when compared to the currently used multi-slice display techniques.

Received Nov. 14, 1989; revision accepted Apr. 4, 1990.

For reprints contact: Dr. G. Lamoureux, Professeur Agrégé, Département de Médecine Nucléaire et Radiobiologie, CHUS, 3001, 12e Avenue Nord, Sherbrooke, P. Québec, J1H 5N4.

MATERIALS AND METHODS

Patients

Seventeen normal right-handed male subjects recruited from the normal control pool of the UCSD-Mental Health Clinical Research Center, ranging in age from 25 to 55, constituted the study group. All of them received a physical and laboratory examination, a structured psychiatric interview and the schedule for affective disorders and schizophrenia (SADS). All were free of significant developmental, medical, or psychiatric disorders. No subject had a history of loss of consciousness lasting longer than 5 min or one which resulted in neurologic sequelae. All subjects were free from illicit drugs and medication, refrained from drinking alcohol for 7 days prior to the study, and from caffeine and tobacco the day of the study. The subjects reported to the Department of Nuclear Medicine of the Veterans Administration Hospital of San Diego early in the morning. The subjects reclined on the imaging table in a quiet, dimly lit room and were instructed to keep their eyes closed but to remain awake. An i.v. was started in an arm vein. The syringe, containing 3–4 mCi of [^{123}I]IMP, was imaged at a fixed distance from the collimator of the gamma camera for a total time of 1 min immediately prior to the injection. At the end of injection, the syringe was flushed several times to assure that the entire dose had been administered. The first tomographic acquisition (SPECT) began 20 min postinjection. Subsequent acquisitions began 2 and 4 hr after the injection without specific control of subject behavior between the scans.

Imaging Protocol

All of the patients were scanned with a truncated head General Electric 400 AT-Starport camera (Milwaukee, WI) and the tomographic data reconstruction was carried out on a GE-Star II computer system. To assess the quality of the camera, a 30-million count intrinsic flood was acquired each morning with a 0.7-mCi technetium-99m (^{99m}TC) source located precisely five useful fields of view away (2.0 meters) on the central axis of the detector. This quality control was

initially performed with an ^{123}I source, but no appreciable difference could be found between the ^{99m}Tc source and the ^{123}I source. The flood image was processed on the computer and a report generated containing the integral uniformity as well as a measure of the standard deviation from pixel to pixel within the useful field of view. These values were plotted on a graph to keep track of the stability of the camera from day to day.

The isotropy (sensitivity and parallelism) of the high resolution, low-energy collimator was initially assessed (*13*) and found not to introduce any appreciable nonuniformity in the reconstructed images. This evaluation took into account the low count levels typically obtained in an [^{123}I]IMP brain study. The center of rotation was determined on a monthly basis according to the manufacturer's recommendation.

The tomographic acquisition data consisted of 96 views (64 × 64 matrix), with a zoom of 1.3 (pixel size: 4.8 mm × 4.8 mm), covering a 360-degree counterclockwise elliptical orbit around the patient. The starting position for this orbit was constantly the right side of the brain and the frontal area was imaged last. The counting time for each view was set at 15 sec in order to keep the total scanning time within 35 min. Repeat scans beginning at 2 and 4 hr were performed in a similar manner.

Reconstruction of the Data

Tomographic reconstruction was carried out on a GE-Star II computer system. The raw data was pre-filtered with a two-dimensional Butterworth filter with a power of 11.0 and a cut-off frequency of 0.35 cycles/centimeter. Count rate attenuation due to absorption by soft tissues and bone was corrected for, assuming a uniform effective attenuation coefficient of 0.11/cm and an elliptical contour fitted individually, for each transaxial slice, on an isoactive contour set at 15% of the maximal count within the entire brain.

The transaxial slices were reconstructed using a distance-weighted backprojection algorithm [Nowak reconstruction algorithm (*14*)], readily available on the Star II system. The sagittal and coronal slices were generated from these data.

A complete orthogonal set of reoriented slices was then produced after defining a new transaxial plane on a mid-sagittal image (Fig. 1). This two-step procedure began with the definition of a proper mid-sagittal plane on the original transaxial images (correction for any axial rotation of the head). Then, a new transaxial plane was defined by drawing a straight line running from just under the frontal lobe to a point halfway between the occipital lobe and the cerebellum on this mid-sagittal slice (Fig. 1B). The new coronal plane was automatically defined by the previous two operations.

Quantitative Analysis

Transformation of the reconstructed data and mapping of the cerebral uptake were also carried out on the Star II system, using the "Advanced Programmability" (PASCAL) feature. This process required ~30 min of computer time for each tomographic study.

The reconstructed data was first normalized to take into account the exact dose administered to each patient. The number of counts in each voxel of the reconstructed volume, which is proportional to the activity in the corresponding location of the brain of the subject under examination, was multiplied by a normalization factor (N), which was calculated from the number of counts (C) in the image of the syringe obtained immediately before the injection. More specifically:

$$N = 500{,}000 / C.$$

Typically, this normalization factor was approximately equal to 1, since the number of counts (C) recorded over 1 min with a 4.0-mCi dose of IMP was approximately equal to 500,000. Since the actual number of counts recorded was dependent on the exact dose administered to each patient multiplied by the sensitivity of the system, this one-step procedure corrected for variation in both of these two parameters. The number of counts found in each voxel after applying this normalization process was further corrected for physical decay on the basis of the time elapsed between injection and the beginning of the tomographic procedure. The resulting number of counts in each voxel was then directly proportional to the uptake of each individual volume element, expressed in some arbitrary units.

The mapping technique we have developed to present those results is similar in many respects to the technique used by geographers to depict the surface of the earth, either with an

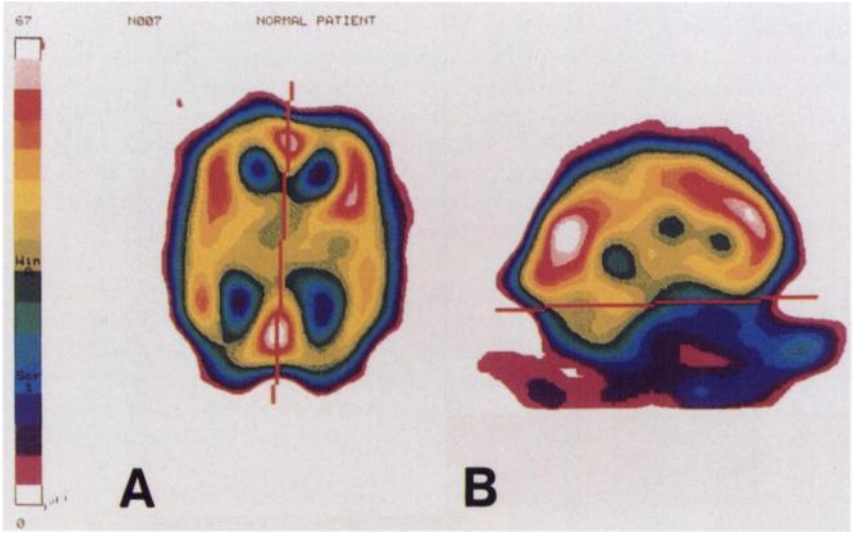

FIGURE 1
Reorientation of the slices. (A) Definition of an appropriate mid-sagittal plane on a transaxial slice, followed by (B) the definition, on a reoriented mid-sagittal slice, of a new transaxial plane tangent to the under portion of the frontal and occipital lobes.

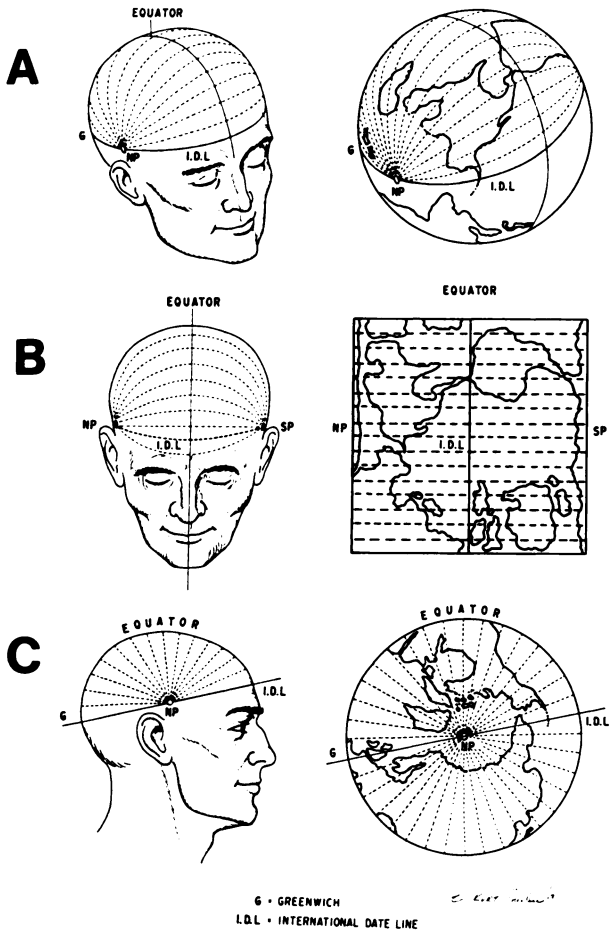

FIGURE 2
Mapping techniques. (A) Borrowing from the geographers a method to represent the surface of a spherical object on a flat paper, we used both equatorial (B) and hemispheric maps (C) to depict the distribution of a radiotracer in the cortex.

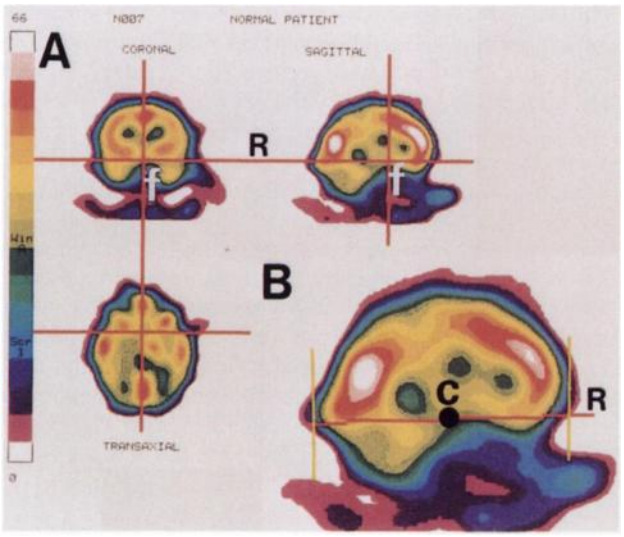

FIGURE 3
Definition of the "center" of the brain. (A) The "center" of the brain (c) was defined as being located on the transaxial plane which was tangent to the undersurface of the brain at the level of the interpeduncular fossa (f). The selection of this "reference plane" (R) was done from the simultaneous display of the reoriented sagittal, coronal and transaxial slices. (B) The exact location of (c) on (R) was determined by the user from the display of a mid-sagittal slice, on which the anterior and posterior limits of the brain were easiest to define (yellow vertical lines).

equatorial map or with two hemispheric maps (Fig. 2), each one corresponding to one hemisphere (northern and southern hemispheres versus right and left sides of the brain). The inner structures of the brain could also be represented in a similar fashion, in analogy with the peeling of an onion, each "layer" being represented by additional uptake maps.

To facilitate the extraction of the pertinent data and the creation of our maps, we applied a spherical transform to the SPECT data, rather than the cylindrical transform reported by Ichise and Crisp (*15*). This meant that the information on the uptake of each volume element of the brain, which is normally expressed in terms of its (x,y,z) coordinates, x and y referring to the coordinate within a slice and z, referring to the slice number, had to be expressed in terms of three other coordinates (r, Θ, and ϕ) after definition of a center of reference.

The first step of this transformation was the selection of an appropriate "center" of reference. The "center" of the brain (c) was defined anatomically (Fig.3) as a point located halfway from side to side of the brain (mid-sagittal) and halfway from the front to the rear on a transaxial plane ("reference plane," R), arbitrarily defined as the one tangential to the undersurface of the brain at the level of the interpeduncular fossa (apparent recess located between the two temporal lobes on a coronal slice). This "center" was easily defined by the user from the simultaneous display of the reoriented sagittal, coronal and transaxial slices. A transverse axis extending from one side of the brain to the other, through this "center," was referred to as the "central axis" (ca) of the brain.

Given that center of reference, the spherical transform allowed us to represent the data contained in the entire set of transaxial slices in terms of three coordinates (Fig. 4): "latitude" (ϕ), "longitude" (Θ), and radius (r). The longitude of a voxel was the angle formed by the anterior half of the "reference plane" (R) and the "voxel plane" (P) defined by the voxel itself and the "central axis." The "latitude" of a voxel was defined as the angle between the right half of the "central axis" and the radius (r) connecting that pixel to the "center" of the brain. So defined, the "longitude" could vary by 360° and the "latitude" by 180° (unlike the geographic model where the longitude is expressed in terms of degree east or west of Greenwich, and the latitude, in terms of degree north or south of the equator, the mid-sagittal line in our model).

With this transformation, the frontal area had a longitude (Θ) grossly comprised between 0° and 90°, while the cerebellum was located at a longitude slightly over 180° relative to the anterior half of the "reference plane." In a half-plane having a longitude of 90°, (similar to the upper part of a mid-coronal slice), the right temporal lobe had a latitude (ϕ) of 0°, the mid-sagittal line was located at 90°, and the left temporal lobe was at 180°.

Sampling of the transaxial data was done at 64 values of longitude covering the 360° around the "central axis" of the

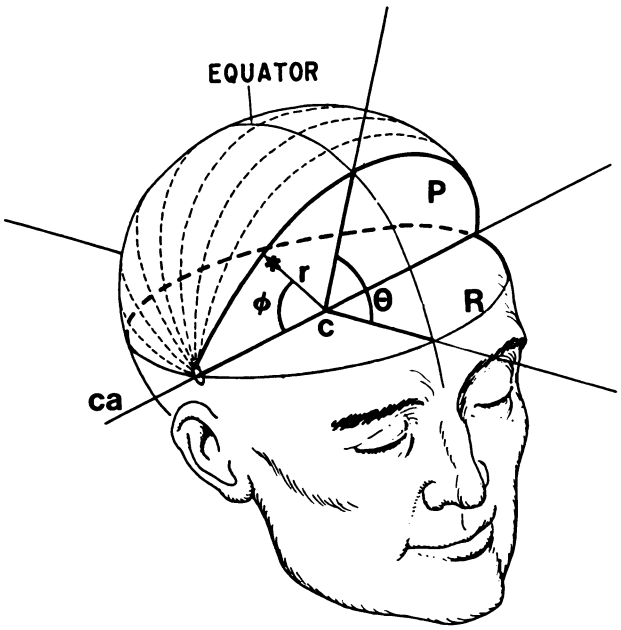

FIGURE 4
Definition of a new reference system. The location of any voxel (*) within the reconstructed volume was described by its latitude (ϕ), longitude (Θ), and distance (r) from the "center" of the brain (c). The exact coordinates of that voxel located on the "pixel plane" (P) were uniquely defined by the definition of the "central axis" (ca) of the brain [transverse axis through (c)] on the "reference plane" (R).

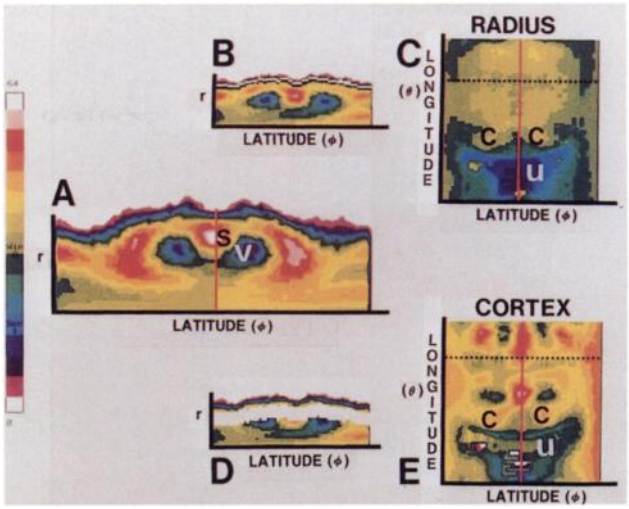

FIGURE 5
Data extraction. (A) One of 64 images of the uptake (color coded) as a function of latitude (ϕ) and radius (r), after transformation of the data. The ventricles (v) and the mid-sagittal sinus (s) are easily recognized. (B) Outer surface of the brain as defined by an isoactive contour (white line) drawn on each image. The y-coordinate of each pixel in that line correspond to the radius of the brain at a given latitude (ϕ = x-coordinate) and longitude (Θ = image #). (C) "Equatorial" map of the radius of the brain (color coded) displayed in terms of the latitude (ϕ) and longitude (Θ). The symmetric shape of this brain can readily be appreciated as well as the extent of the area corresponding to the undersurface of the brain (u). Our definition of the cortical layer of the brain is depicted by the white area in (D). (E) "Equatorial" map of the cortical uptake, in correspondence with the "equatorial" map of the radius (C). The horizontal dotted lines in (C) and (E) were drawn at the longitude of the image presented in (B) and (D).

brain. At each longitude, the data were sampled 64 times to cover the range of latitude from 0° to 180° (from the right temporal area to the left temporal area). Radial sampling was performed at each of these 4,096 combinations of latitude and longitude at 32 points (equivalent to 32 voxels) thus covering the entire volume of a sphere (larger than the brain) having a diameter equal to the width (64 voxels) of the original data. The transformed data could then be represented in a set of 64 images (one for each longitude) of 64 × 32 voxels (64 values of latitude and 32 values of radius). This set of images (Fig. 5A) constituted the basis of any further analysis. It should be remembered that the number of counts in each voxel within this set of images remained proportional to the uptake in the volume element corresponding to its coordinates.

The "outer surface" of the brain was defined as an isoactive surface defined by the first voxel whose value exceeded a predefined threshold when moving radially from the extremity of each radius toward the center of the brain (Fig. 5B). The radius of the "outer surface" could easily be obtained from the above data and the resulting information could be displayed in a 64 × 64 image ("equatorial map") where each pixel (Fig. 5C) was color-coded to represent the radius at that latitude (x-axis) and longitude (y-axis). A threshold value of 30% of the maximal voxel count was used in our protocol. With some experience, the shape of the patient's brain and/or the proper definition of the "center" of the brain could be ascertained from the symmetry of the radius map.

Once the outer surface of the brain had been defined, the brain could literally be peeled and a map of the uptake within that "peel" (uptake versus latitude and longitude) could be displayed. The "cortical peel" was defined as that constant thickness region (five voxels thick) whose outer surface was located at 90% of the radius for each latitude and longitude (Fig. 5D). By this procedure, we defined a volume located just below the isoactive outer surface of the brain with a constant thickness of 2.40 cm.

An "equatorial map" of the cortical uptake averaged over the chosen thickness (average counts/voxel) could then be generated and displayed using a chromatic color scale (Fig. 5E) with 16 discrete levels. Since the data have been corrected for the injected dose as well as for physical decay, this color scale could be kept constant for all subjects. It must be noted that on these equatorial maps (longitude versus latitude), the mid-sagittal line was represented by a vertical line (constant "latitude" of 90°), in analogy with an equatorial map of the earth where the equator is represented by a straight (although horizontal) line.

Alternatively, in order to reduce the distortion introduced by the equatorial maps in the polar area (temporal lobes in the case of the brain), a set of "hemispheric maps" was generated from the same data (Fig. 6). On these hemispheric maps, the mid-sagittal line was located at the periphery of a radial display, where the radius represents the latitude, while the angular position of each point represented the longitude from 0° to 360°. The right hemispheric map covered a range

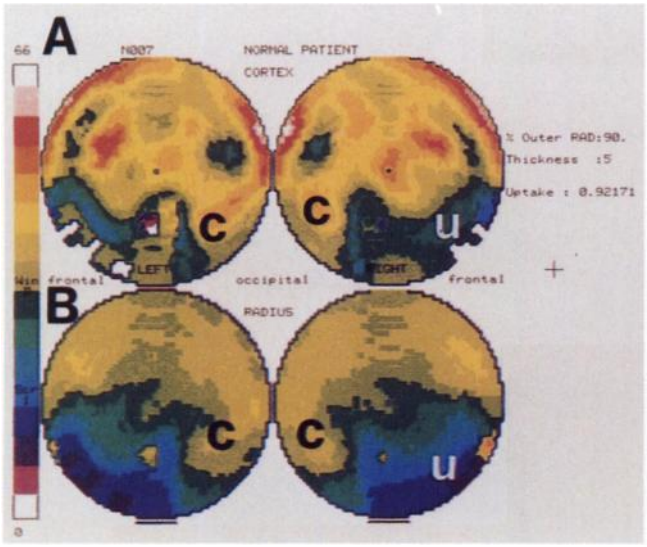

FIGURE 6
Hemispheric maps. The data contained in each "equatorial" map was represented on two "hemispheric" maps in correspondence with the two brain hemispheres. Again the cerebellum (c) and the area corresponding to the undersurface of the brain (u) can readily be identified on these maps of the cortical uptake (A) and of the radius (B).

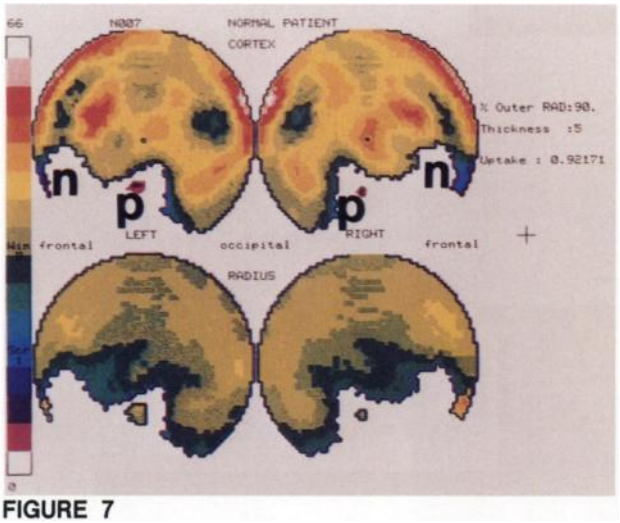

FIGURE 7
Threshold on the radius. The area corresponding to the undersurface of the brain was discriminated on the basis of its lower radius. Whenever the radius fell below a predefined threshold (≈6.0 cm), the pixel was eliminated both from the uptake (A) and the radius maps (B). The activity measured within the parotid glands (p) could not be discriminated against on the basis of its distance from the center of the brain. The activity within those glands as well as within the nasopharyngeal area (n) was sufficiently high to introduce an error in the automatic determination of the contour of the brain.

of "latitude" varying from 0° in the center to 90° on the periphery, while the left hemispheric map covered the range from 90° in the periphery to 180° in the center.

When the hemispheric maps of the cortical uptake were displayed along with the hemispheric maps of the radius of the brain, it became evident that a large portion of them did not represent the outer cortex but the uptake in structures underneath the brain, or even external to the brain (e.g., salivary glands). However, these structures could be excluded on the basis of the shorter radius of the brain in these directions. The hemispheric maps of the cortex were thus left blank (pixels set to zero) wherever the radius in the corresponding radius map was below a predefined threshold (Fig. 7). The similarity of these uptake maps to lateral views of the brain is evident, yet the number of counts in each pixel (color-coded) really represent the uptake of the tracer as a function of the angular position of each specific volume element of the "cortical peel," around the "center" of the brain.

The mean absolute "cortical uptake" of a tracer was calculated from the average value of the uptake (pixel counts) in the left and right hemispheric maps of the "cortical layer," limited to those values with a longitude between 0° and 180°. This area covered grossly the two hemispheres and excluded the cerebellum. This average value (pixel counts) was further divided by 48, somewhat arbitrarily, in order to reduce the normal value of the mean "cortical uptake" in the vicinity of 1 (arbitrary uptake unit: Uu). On an absolute basis, the Uu we used to express this average cortical uptake was found to be equal to 3.62×10^{-3}% of the administered dose/cc (see Appendix).

Finally, it must be noted that, by definition, the calculation of the mean "cortical uptake" was independent of the exact brain size of each individual.

RESULTS

"Cortical uptake" values were obtained in 17 individuals at 20 min, 2 hr, and 4 hr after injection of IMP (Table 1). These results suggest a slow clearance of the tracer (paired t-test with a $p < 0.01$) from the cortical layer, over time, with a mean uptake (±s.d.) of 0.921 (±0.185) at 20′, decreasing to 0.803 (±0.107) at 120′, and finally down to 0.748 (±0.103) at 240′ (Fig. 8). Within our age range, no significant correlation was found between the measured uptake at each time period and the age of the subject.

To appreciate how well these results could be reproduced, 10 subjects (Table 1) had a repeat study performed at a later date (2 wk–9 mo). A paired t-test (initial study versus repeat study) analysis of the uptake values obtained at 120′ and 240′ resulted in p values of 0.29 and 0.14, respectively, indicating no demonstrable difference between the first and second series of measurements ($p > 0.1$). However, the same test performed on the 20′ uptake values resulted in a p value of 0.05, suggesting a difference between the two series of measurements. A more detailed look at the uptake values obtained from this restricted group suggests that these values are different in their mean and, perhaps more strikingly, in their standard deviation around the mean (Fig. 9).

To further assess the distribution of the tracer in the cortex, a composite uptake map was generated by adding together the maps of all the subjects and by dividing

TABLE 1
Cortical Uptake Values

Subject	Age	First study			Repeat study		
		Time after injection			Time after injection		
		20′	120′	240′	20′	120′	240′
1	55	1.054	0.917	0.832	0.945	0.968	0.846
2	55	0.878	0.795	0.812			
3	47	0.843	0.666	0.656			
4	46	0.909	0.846	0.753	0.762	0.716	0.707
5	46	1.108	0.884	0.837	0.926	0.848	0.839
6	46	0.829	0.927	0.860			
7	43	1.007	0.677	0.757	0.944	0.818	0.696
8	42	0.852	0.809	0.757	0.918	0.904	0.765
9	41	0.853	0.840	0.654	0.677	0.617	0.575
10	37	0.717	0.645	0.582	0.737	0.661	0.629
11	37	1.460	0.994	0.911	1.209	0.782	0.710
12	35	0.901	0.823	0.818			
13	34	0.984	0.736	0.685			
14	31	0.577	0.609	0.587	0.740	0.689	0.546
15	30	0.876	0.878	0.846			
16	29	0.938	0.835	0.759			
17	25	0.875	0.776	0.603	0.821	0.763	0.676
Mean (17 subjects)		0.921	0.803	0.748			
s.d.		0.185	0.107	0.103			
Mean (10 subjects who had a repeat study)		0.924	0.800	0.727	0.852	0.777	0.699
s.d.		0.236	0.124	0.116	0.152	0.111	0.100

the integral value in each pixel of the resulting image by the total number of subjects.

Again, the number of counts in each pixel of these composite maps must be thought of as an absolute measure of the mean uptake among these normal subjects, within that small but specific region of interest located, within the 2.40-cm thick "cortical layer" of the brain, at the latitude and longitude given by the coordinates of the pixel. If those values are displayed with a 16-level color scale which is kept constant in range, then each color will represent a specific absolute uptake range. This is why a constant range of 0 to 64 counts/pixel was used in Figures 10A, 11A, and 12A.

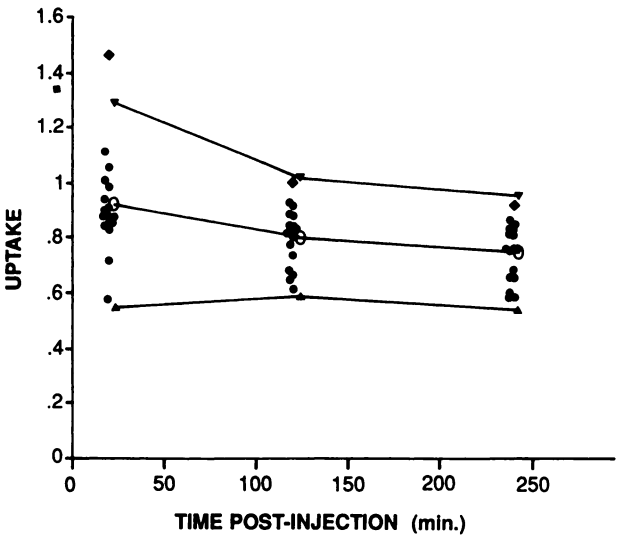

FIGURE 8
This graph of the cortical uptake as a function of time after injection illustrates the average washout of [^{123}I]IMP from the cortex of our subjects. By definition, most of the individual uptake values (.) fell in the range defined by the average (o) ± 2 s.d. (▲ and ▼) except for Subject 11 at 20′ after injection. For some yet unknown reason, the uptake of Subject 11 (◆) was more than 4.5 s.d. higher than the average of the other subjects.

The composite cortical uptake maps obtained at 20 min, 2, and 4 hr postinjection are shown in Figure 10A. Since these maps were fairly symmetric from one hemisphere to the other, only the right hemisphere is represented. The absolute scales for the maps obtained at 2 and 4 hr were modified by a factor of 1.15 and 1.23, respectively, to compensate for the overall washout of the tracer over time, thus giving a better appreciation of the fact that the uptake is becoming more uniform with time. Also presented in this figure (Fig. 10B) are the maps corresponding to the standard deviation measured at each location of the cortex. The standard deviations were expressed as percent of the uptake in the corresponding location of the cortex and is color-coded on a scale ranging from 0%–32% (2% per color level).

The average washout at each location of the cortical layer was obtained by subtracting the composite maps one from the others. The absolute cortical uptake maps, presented on the same scale, and the wash-out measured at each location from 20′ to 120′ and from 20′ to 240′ are presented in Figure 11. The wash-out at each loca-

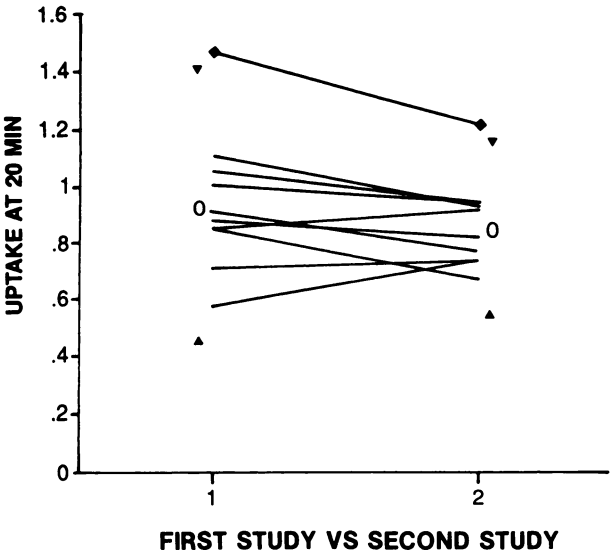

FIGURE 9
This graph illustrates on an individual basis the relation between the 20′ uptakes measured on two separate occasions, 15 days to 9 mo apart. The mean uptake at 20′ (o) of the 10 patients was slightly diminished and the variation in their uptake values [±2 s.d. (▲ and ▼)] was much reduced the second time around. Subject 11 (◆) shows a similar behavior in that respect but his uptake was still very high the second time.

tion is expressed as percent of the initial activity and is color-coded on a scale of 0%–64% (4% per color level).

DISCUSSION

Until recently, it was felt that functional brain imaging was the exclusive territory of positron emission tomography (PET) due to the wide choice of physiologically specific positron emitting tracers and its well proven quantitative ability. Even though the new clinically available radiopharmaceuticals for SPECT imaging are limited to the study of "blood flow," several investigators have already shown their potential in the study of many pathologic states that will result in a qualitatively abnormal cerebral study (*6–12*, *16–18*). As pointed out by Holman (*19*) in 1987, quantitative SPECT imaging is within our reach and should become a reality if we want to take full advantage of those results in the day to day evaluation of CNS disease. Given the various tracers currently in development, quantitative SPECT imaging could even become a powerful, yet readily accessible research tool leading to new clinical applications.

The potential value of our method for the absolute measurement of the cortical uptake of a tracer either globally (uptake values) or locally (uptake maps) is well illustrated by this study of the cortical uptake and distribution of [^{123}I]IMP in a group of normal subjects.

Among other things, these results clearly indicate the risks associated with a relative measure of the uptake based on an "internal standard," defined as the maximum or average activity measured within the cerebellum which we have shown to be an area where the variations in absolute uptake and the washout are the highest (Fig. 10B and 11B).

However, the measurement of the absolute cortical uptake of a tracer is certainly not by itself the ultimate answer to all the problems related to the evaluation of brain physiology. The particular behavior of Subject 11 (Table 1) is very interesting in this respect. His cortical uptake at 20′ was fairly high on both the initial and the repeat study, with a value of 1.460 and 1.209, respectively, as compared to a mean uptake of 0.887 (±0.126) for the 16 other subjects on their first study, and 0.830 (±0.105) for the 9 others subjects who had a repeat study. Indeed, these values contributed significantly to the standard deviation obtained on the 20′ uptake values. At 120′ and 240′, however, his uptake was within normal range (Fig. 8). Further experience with this technique in normal patients should tell us whether

FIGURE 10
(A) Composite uptake maps. The hemispheric uptake maps of the subjects were added together to produce those composite maps depicting the cortical distribution (right hemisphere) of the tracer at 20′, 120′, and 240′ respectively. To fully appreciate the more even distribution of the tracer over time, the scale of each image was adjusted to compensate for the measured global washout (see Table 1). (B) The standard deviation in the cortical uptake was measured for each pixel. The results, expressed as a percentage of the local uptake, are presented in those maps (2% per color level). The high uncertainty in the absolute uptake measured at the level (c) of the cerebellum (≅17%) can be readily appreciated.

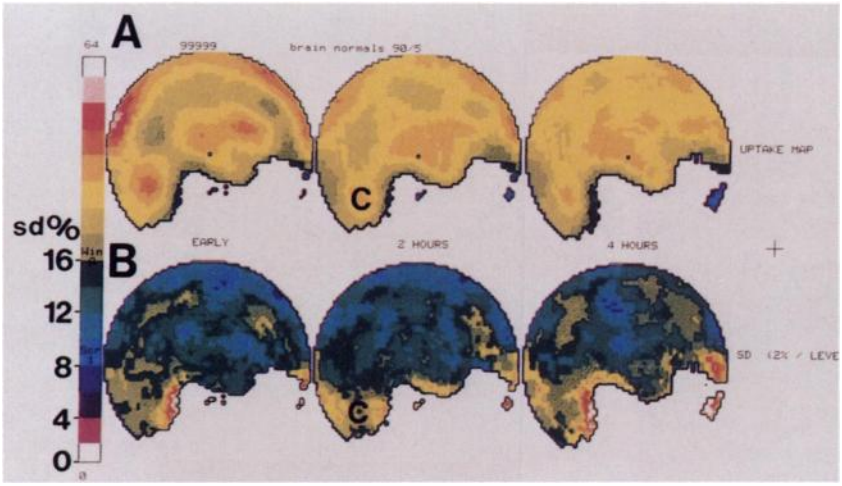

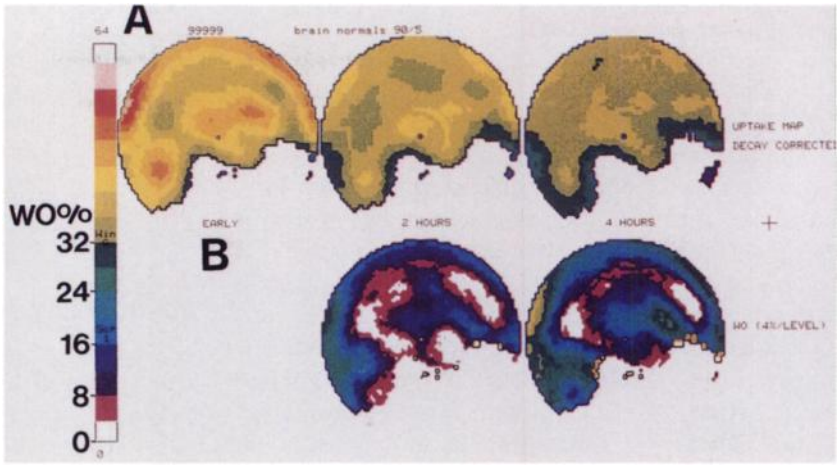

FIGURE 11
(A) The composite uptake maps obtained at 20′, 120′, and 240′ are displayed on the same absolute scale to illustrate the washout of the tracer over time. (B) The washout was measured for the 20′–120′ and the 20′–240′ time intervals. The results were expressed as a percentage of the uptake at 20′ (4% per color level). The white areas within those maps are in correspondence with areas where the washout was negligible (<4%). Grossly, the areas of highest uptake initially were also the areas with the highest washout rates. Again, the cerebellum was an area of rapid variations in activity over time.

this observation was only a statistical oddity or a true reflection.

The variations observed in the 20′ uptake values between the initial and repeat study (Fig. 9) are also very intriguing but not without precedent. Prohovnic et al. (*20*) have reported a similar tendency to a relatively lower mean cerebral blood flow and standard deviation in their second measurement on resting subjects with a xenon-133 inhalation technique. This phenomenon was nicely explained by the work of Gur et al. (*21*) showing a curvilinear, inverted-U relationship between anxiety and cerebral blood flow. Such an observation could perhaps even explain the extremely high 20′ uptake of Subject 11 on his first visit, which reverted toward normal in the repeat study.

In a different perspective, the standardization in the presentation of the results offered by this mapping technique could simplify the analysis of the distribution of a tracer in the cortex of one individual or group of patients in terms of the normal values depicted by the composite (normal) average maps (Fig. 10A).

The left hemispheric uptake map of a normal subject and the right hemispheric map of a patient with a huge frontal stroke showing a recent progression of his dementia are presented side by side in Figure 12A. The cerebellum of that patient could not be scanned properly due to an important scoliosis, a fact which is clearly depicted in this map. A "percentage analysis" was obtained by dividing those individual uptake maps by the normal composite uptake map and multiplying by 100 (Fig. 12B). The color-coded images showed that the normal subject had an uptake ranging from 75% to 125% of the normal values as compared to the patient who had an uptake reduced below 75% both in the frontal and parieto-occipital areas. Similarly, a "standard deviation analysis" was obtained by subtracting the individual maps from the normal map and then by dividing the result by the standard deviation measured at each location in our normal reference group (Fig. 12C). The color-coded images obtained showed that the normal subject had an uptake comprised between ±1.5 s.d. from the normal average uptake for each area while the patient had an uptake comprised between +0.5 and −2.5 s.d. everywhere except for two areas within the frontal lobe which have a very low uptake by all standards. The uptake in the parietal area is within "normal" limits, those limits being defined as ±2.5 s.d.

The ability to take into account the nonuniform distribution of the tracer and the expected local varia-

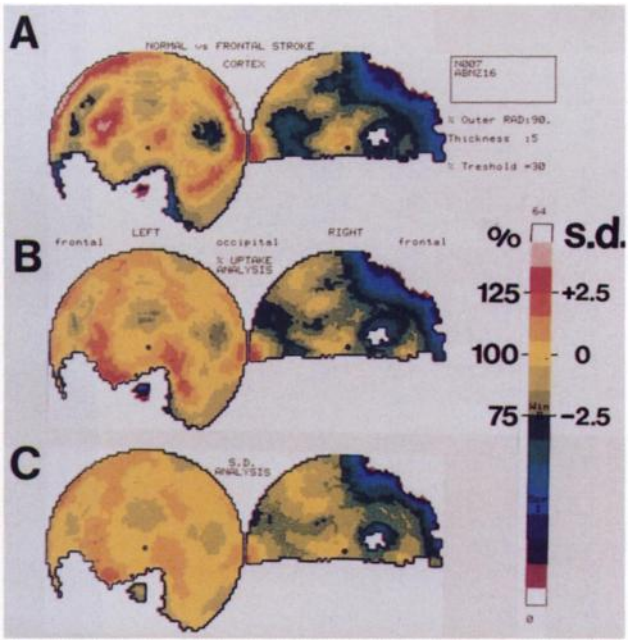

FIGURE 12
(A) Left hemispheric uptake map of a normal subject (left); right hemispheric uptake map of a patient with a frontal stroke (right). (B) Percentage analysis: the individual uptake maps were compared to the normal composite uptake map (Fig. 10A at 20′) and expressed as a percentage (10%/color level; yellow = 95%–105%). (C) Standard deviation analysis: the deviation from normal uptake also was expressed in terms of the standard deviation measured at each location (1 s.d./color level; yellow = normal average uptake ±0.5 s.d.).

tions in uptake should be a strong asset for these or similarly derived analysis techniques.

CONCLUSION

The program described in this paper offers several advantages to the nuclear medicine practitioner. First, this mapping technique is a powerful data reduction tool that allows contiguous areas of the brain (e.g., the cortex) to be evaluated without having to mentally integrate from slice to slice. Second, this quantification technique has proved to be reliable with [^{123}I]IMP and could result in the development of quantitative diagnostic criteria. Such an approach would remove much of the subjectivity involved in the evaluation of the distribution of these tracers.

APPENDIX

Calculation of the (% dose/cc) Equivalent to 1.0 Uu (Our Arbitrary Uptake Unit)

The basis for these calculations, namely that:

$$\text{Number of counts in reconstructed object} = \text{SUM}\left(\begin{array}{c}\text{counts in each}\\ \text{projection}\end{array}\right) \quad (1)$$

was validated with a simulation program allowing us to generate the 96 projections of a point source with a known activity which were then backprojected using the Nowak reconstruction algorithm.

Assuming that the activity recorded by the camera during our preliminary image of the syringe containing the total administered dose of IMP was 500K cts/60 sec (which was the purpose of our normalization process), the total number of counts (N) that would have been recorded during a tomographic acquisition of a point source containing the entire dose would then have been, according to our acquisition protocol:

$$N = \frac{500\text{K counts} \times 96 \text{ views} \times 15 \text{ sec/view}}{60 \text{ sec}} = 12{,}000 \text{ counts.} \quad (2)$$

This means that if the entire dose administered to the patient could have been fitted within a single voxel, this voxel containing 100% of the dose would have registered 12,000 counts.

By definition, the voxels corresponding to the "cortical layer" of the brain were said to have an average uptake of 1 Uu, our arbitrary uptake unit, if the average number of counts per voxel was equal to 48 counts. This number of counts per voxel could be related to the administered dose in the following way:

$$1.0 \text{ Uu} = 48 \text{ counts/voxel} \quad (3)$$

$$= \frac{48 \text{ counts/voxel} * 100}{12{,}000 \text{ counts/dose}} \quad (4)$$

$$= 4 \times 10^{-4} \text{ \%dose/voxel} \quad (5)$$

$$\text{But since 1 voxel} = (0.48 \text{ cm})^3 \quad (6)$$

$$1.0 \text{ Uu} = 3.62 \times 10^{-3} \text{ \%dose/cc} \quad (7)$$

One basic assumption underlying these calculations is that the data were properly corrected for attenuation. The accuracy of the attenuation correction method, which is part of the GE tomographic software package, was not evaluated. However, we can assume that it was, at best, only a first-order approximation to the difficult problem of attenuation and scattering. This certainly did limit the precision of our absolute measurements (systematic error) but it should not have affected the reproducibility of our results (random error).

ACKNOWLEDGMENTS

The authors thank Dr. J.C. Gillin for his help and encouragement, as well as for his constant assistance in the recruitment and evaluation of the subjects.

The authors also thank Dr. J.P. Tétreault for his advice on the statistical analysis of the results, K. Smolen and M. Buist for their graphic assistance, and the entire staff of the Nuclear Medicine Department of the V.A.M.C. of San Diego for their technical support.

In addition, the contribution of Medi-Physics and the assistance for product support by B.A. Salsitz and Dr. J.D. Miller are gratefully acknowledged.

This research was performed at the Veterans Administration and University of California, San Diego while Dr. Lamoureux was on sabbatical from the University of Sherbrooke.

This work was supported in part by the Veterans Administration Research Training Grant in Psychiatry, by the NIMH grants MH30914 and MH18399, and by gift account #444-873-48-430 (budget #2208).

REFERENCES

1. Hill TC, Holman LB, Lovett R, et al. Initial experience with SPECT (single-photon computerized tomography) of the brain using N-isopropyl I-123-p-iodoamphetamine: concise communication. *J Nucl Med* 1982; 23:191–195.
2. Leonard J-P, Nowotnik DP, Neirinckx RD. Technetium-99m-d,l-HMPAO: a new radiopharmaceutical for imaging regional brain perfusion using SPECT—a comparison with iodine-123-HIPDM. *J Nucl Med* 1986; 27:1819–1823.
3. Holman BL, Hellman RS, Goldsmith SJ, et al. Biodistribution, dosimetry, and clinical evaluation of technetium-99m-ethyl cysteinate dimer in normal subjects and in patients with chronic cerebral infarction. *J Nucl Med* 1989; 30:1018–1024.
4. Kung HF, Pan S, Kung M-P, et al. In vitro and in vivo evaluation of [I-123]IBZM: a potential CNS D-2 dopamine receptor imaging agent. *J Nucl Med* 1989; 30:88–92.
5. Mertens J, Bossuyt-Piron C, Guns M, Bossuyt A, Leysen J, Janssen C. High selective serotonin S_2 receptor mapping with SPECT in baboon brain. *J Nucl Med* 1989; 30:741.
6. Hill TC, Magistretti PL, Holman BL, et al. Assessment of regional cerebral blood flow (rCBF) in stroke using SPECT and N-isopropyl-(I-123)-p-iodoamphetamine (IMP). *Stroke* 1984; 15:40–45.
7. Defer G, Moretti J-L, Cesaro P, Sergent A, Raynaud C, Degos J-D. Early and delayed SPECT using N-isopropyl-p-iodoamphetamine iodine-123 in cerebral ischemia. A prognostic index for clinical recovery. *Arch Neurol* 1987; 44:715–718.
8. Raynaud C, Rancurel G, Tzourio N, et al. SPECT analysis of recent cerebral infarction. *Stroke* 1989; 20:192–204.
9. Lambert R, Gilday DL, Ash JM, Hwang PA, Kern RZ, Ogunmekan AD. Interictal SPECT-HMPAO and epilepsy in children. *J Nucl Med* 1988; 29:792.
10. Park HM, Shen W, Worth RM, Markand ON, Wellman HN,

Lee BI. I-123-HIPDM-SPECT for selection of ideal candidates with refractory complex partial seizures (CPS) for surgery. *J Nucl Med* 1989; 30:751.
11. Sharp P, Gemmell H, Cherryman G, Besson J, Crawford J, Smith F. Application of iodine-123-labeled isopropylamphetamine imaging to the study of dementia. *J Nucl Med* 1986; 27:761–768.
12. Cohen MB, Graham LS, Lake R, et al. Diagnosis of Alzheimer's disease and multiple infarct dementia by tomographic imaging of iodine-123-IMP. *J Nucl Med* 1986; 27:769–774.
13. Lamoureux G, Verba J, Halpern SE. A technique for the evaluation of the collimators used for SPECT. *J Nucl Med* 1989; 30:894.
14. Nowak DJ, Fisher RL, Fajman WA. Distance-weighted backprojection: a SPECT reconstruction technique. *Radiology* 1986; 159:531–536.
15. Ichise M, Crisp S, Wortzman G, Kirsh JC, Shapiro BJ. A technique of cortical peeling and mapping by Tc-99m-HMPAO brain SPECT. *J Nucl Med* 1988; 29:914.
16. Raynaud C, Rancurel G, Samson Y, et al. Pathophysiological study of chronic infarcts with I-123 isopropyl iodoamphetamine (IMP): the importance of periinfarct area. *Stroke* 1987; 18:21–29.
17. Johnson KA, Mueller ST, Walshe TM, English RJ, Holman BL. Cerebral perfusion imaging in Alzheimer's disease. Use of single photon emission computed tomography and iofetamine hydrochloride I-123. *Arch Neurol* 1987; 44:165–168.
18. Gemmel HG, Sharp PF, Besson JAO, Ebmeier KP, Smith FW. A comparison of Tc-99-HM-PAO and I-123-IMP cerebral SPECT images in Alzheimer's disease and multi-infarct dementia. *Eur J Nucl Med* 1988; 14:463–466.
19. Holman BL. SPECT of the brain and heart—future directions. *J Nucl Med* 1988; 29:567–570.
20. Prohovnik I, Hakansson K, Risberg J. Observations on the functional significance of regional cerebral blood flow in "resting" normal subjects. *Neuropsychologia* 1980; 18:203–217.
21. Gur RC, Gur RE, Resnick SM, Skolnick BE, Alavi A, Reivich M. The effect of anxiety on cortical cerebral blood flow and metabolism. *J Cereb Blood Flow and Metab* 1987; 7:173–177.